

## Measurement of temperature after collision of microparticles with a solid state material

<sup>1</sup>T.Miyachi, <sup>1</sup>M.Fujii, <sup>1</sup>O.Okudaira, <sup>2</sup>S.Takechi, <sup>2</sup>A.Kurozumi, <sup>2</sup>S.Morinaga, <sup>2</sup>Y.Kawachi,  
<sup>2</sup>Y.Shinohara, <sup>3</sup>H.Shibata, <sup>4</sup>M.Kobayashi, <sup>5</sup>H.Ohashi, <sup>6</sup>H.Matsumoto, <sup>7</sup>T.Iwai, <sup>8</sup>K.Nogami

<sup>1</sup>Waseda Univ., <sup>2</sup>Osaka City Univ., <sup>3</sup>Kyoto Univ., <sup>4</sup>Nihon Medical School, <sup>5</sup>Tokyo Univ. Marine  
 Sci.& Tech., <sup>6</sup>JAXA, <sup>7</sup>Univ. Tokyo, <sup>8</sup>Dokkyo Med. Univ.

When a solid state dust/debri detector is used in the future, reliable procedures for analyzing its behavior must be established. The temperature during collision is considered as one of the primary parameters for calibration purpose. However, there have been few studies that have dealt with the temperature during collision.

It is a current interest in establishing a calibration method for a dust detector, one of which is a piezoelectric PZT dust detector onboard the MMO craft. Nevertheless, no reliable theories exist that can explain the PZT signal as a function of velocity.

This note serves to promote calibration technique based on the Planck radiation, by adding some supplements to a report [1].

The amount of energy  $U$  per unit volume radiated at equilibrium with frequency  $\nu$  per unit frequency interval by assuming a blackbody at temperature  $T$  is known.

$$U = 8 \pi h \nu^3 / c^3 [1 / (e^x - 1)], \quad (1)$$

with  $x = h \nu / kT$ , where  $c$ ,  $h$  and  $k$  are the light velocity, Planck constant, and Boltzmann constant, respectively.

Then the number of photons of  $h \nu$  emitted from the blackbody is proportional to a factor  $f$

$$f = (kT/hc)^2 [x^2 / (e^x - 1)], \quad (2)$$

The temperature during collision was exceedingly studied by measuring the absolute number of photons. But there remained a lot of factors that influence on the experimental result; solid angle calculation, reflection of light, fluctuation of the gain control system, emissivity of the radiator and other sources of errors and ambiguities

In order to overcome these difficulties/uncertainties, this report is discussed a method that the temperature can be determined as a function of velocity  $v$ . It is proposed that the relationship between  $T$  and  $v$  can be determined using a photomultiplier as an intermediate standard. This method

needs at least one point where the temperature and velocity values are simultaneously determined. Hereafter this point is called the standard point, at which the temperature and velocity are designated as  $T_0$  and  $v_0$ , respectively. Once the standard point is found, the relation between  $T$  and  $v$  is established with a relative manner.

The amplitude of the photomultiplier output signal  $\tau(T)$  at  $T$  is estimated

$$\tau(T) \propto \int f(x)g \, dx, \tag{3}$$

where  $f(x)$  is represented in eq.(2), and  $g$  is the spectral response characteristic function of the photomultiplier.

On the other hand, the amplitude of the photomultiplier output  $\alpha(v)$  at a velocity  $v$  is experimentally measured. As a result the relation is valid;

$$\tau(T) / \tau(T_0) = \alpha(v) / \alpha(v_0). \tag{4}$$

name	symbol	code
R1081	u	100M
R821	b	200S
R647	v	400K
R1463	w	500U

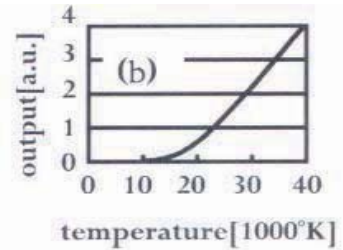
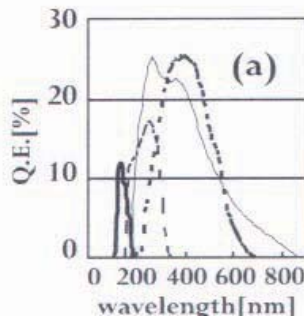


Table I. Four types of photomultipliers. Product name (left), symbolic name (middle) and curve code (right) are listed.

Fig.1(a). Spectral response characteristic functions are plotted: u, b, v, and w are solid-thick dot-thin, solid-thin, and dot-thick lines, respectively.

Fig.1(b). Relative amplitudes using the solid-thick line.  $T_0$  is estimated ~18,000 K by extrapolation.

Four types of photomultipliers (products of Hamamatsu Photonics) were used as listed in Table I. They are designated as u, b, v, and w for convenience. The function  $g$  was measured for each photomultiplier as shown in Fig.1(a).

The u-photomultiplier acts as a threshold detector, because of its narrow window for the wavelength. It works linear over the wide range of temperature. The calculated values are plotted as a function of  $T$  in Fig.1(b). By extrapolating these points, it is estimated to be ~18,000 K at zero amplitude. Accordingly, the temperature at the standard point is  $T_0 \sim 18,000$  K.

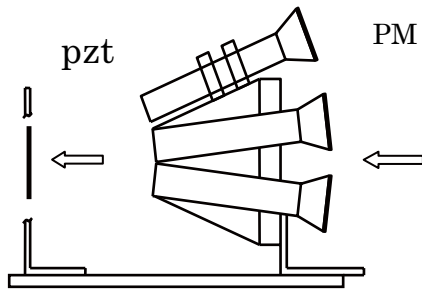


Fig.2. Concept of arrangement.

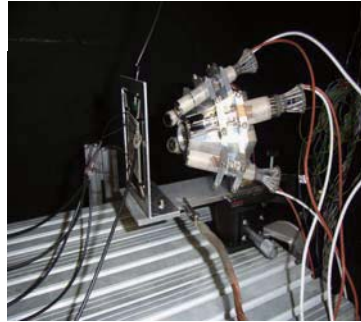


Fig.3. Assembly of photomultipliers.

The five photomultipliers were arranged as conceptually shown in Fig.2. They were assembled as in Fig.3. They were directed toward a PZT element placed at a distance of 60 mm. Two v-type photomultipliers were used; one ( $v_1$ ) was used to measure the flashes and the other ( $v_2$ ) was used as a monitor. All the photomultipliers were biased such that the amplitudes of the output signal were less than 150 mv in order to avoid a possible deviation from linearity.

The PZT element of dimensions of  $40 \times 40 \times 1 \text{ mm}^3$  was coated with a layer of silver electrode that was several  $\mu\text{m}$  thick.

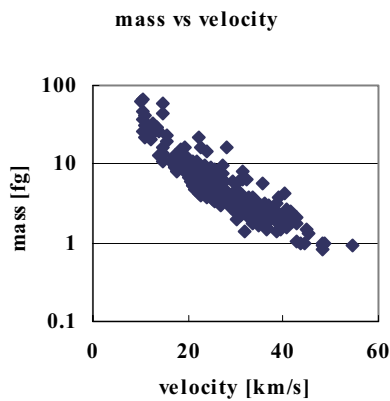


Fig.4. Distribution for the mass and velocity.

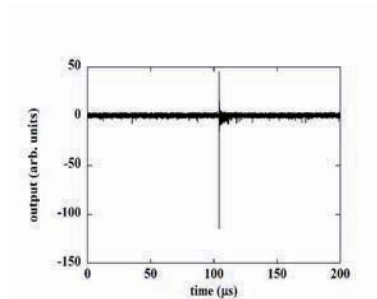


Fig.5. Spike-like form signal.

The hypervelocity particles comprising Ni and Fe particles were supplied by the Van de Graaff accelerator at the Max-Planck-Institut für Kernphysik. The velocity and mass of each particle were measured by scanning the signals induced in an electrostatic electrode [2]. The distribution for the mass vs velocity is plotted in Fig.4. The particles were located within a circle of  $\sim 10 \text{ mm}$  in diameter at the PZT element [3].

The amplitudes of the output signals of  $u$ ,  $b$ ,  $v_1$ , and  $w$  were directly measured with a digital scope  $S_1$ . The amplitudes from the PZT element were measured by another scope  $S_2$  to confirm the occurrence of collision. The  $v_2$ -signal was monitored on  $S_2$  as a time reference. The maximum overall margin of error was estimated to be 30 %.

Only samples that a spike-like form (Fig.5) is recognized are picked up. The width of the spike-like signal is as short as 10~20 ns. The spike-like form is reduced to, for example, the form of  $v_1$  in Figs.6(a) and (b). There are many small signals after the sharp peak, which are considered as flashes of recombination of plasma particles appearing over several tens  $\mu$ s.

It was very rare that five photomultipliers fired almost free from the influence of secondary dust. It was very often to have events that  $v_1$ -,  $v_2$ -, and  $w$ -signals coexisted, but  $b$ - and/or  $u$ -signals missed.

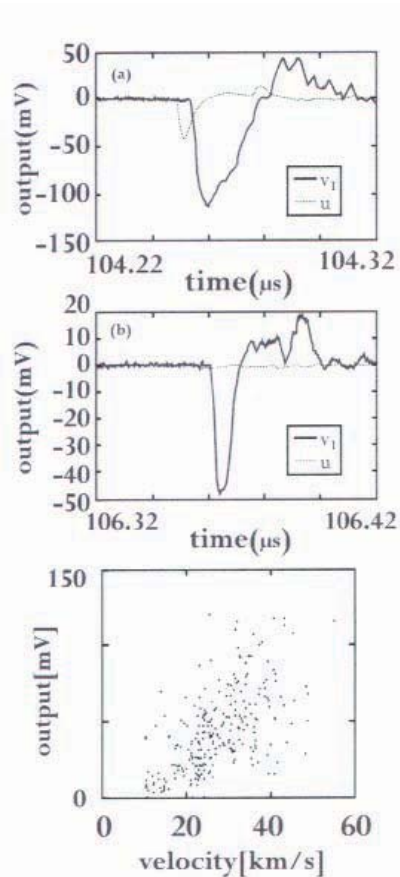


Fig.6.  
 (a) Signal forms belonging to category I.  
 (b) Signal forms belonging to category II.  
 (c) Distribution of the amplitude for the  $v_1$ - photomultiplier.

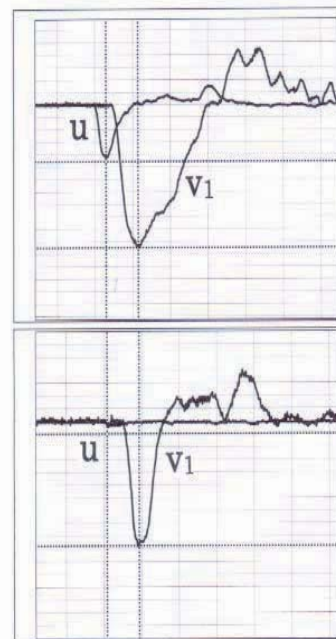


Fig.7. Effect of the screening on the wave form. The details are explained in the text.

The signal form was varied not only among the photomultipliers but also from event to event. Figures 6(a) and (b) shows the typical signal forms observed in the u- and  $v_1$ - photomultipliers. There are some cases in which the signal form appears normal [(a) tagged as category I]. There are various forms that appear irregular [(b) category II]. Such variations are indicative of the wide distribution of the amplitudes [(c) for the  $v_1$ -photomultiplier].

Figures 6(a) and (b) are rewritten in Fig.7. Figure 7 (top) shows that the u-photomultiplier signal is almost normal and follows the  $v_1$ -signal with a time offset of  $\sim 9$ ns. In contrast, Fig.7 (bottom) illustrates that the  $v_1$ -signal is significantly sharp and the u-signal almost disappears at an advanced point in the signal path.

The characteristic behaviors in Fig.6 or Fig.7 can be explained as follows: When a hypervelocity microparticle strikes the PZT element, many secondary particles that screen the photomultipliers from the element are produced. The irregular forms are considered to be a consequence of this screen effect.

The signal forms in Fig.7 (top) belong to category I, while those in Fig.7 (bottom) belong to category II. Similar distributions in Fig.6 (c) were observed in other photomultipliers.

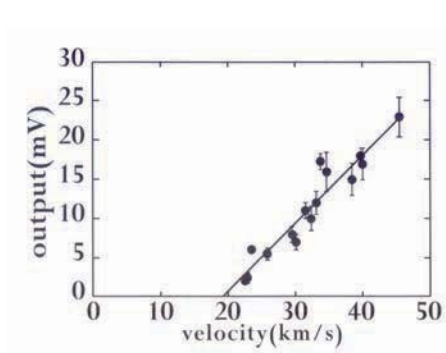


Fig.8. Amplitudes of the u-photomultiplier output signal. The measured points are extrapolated by the solid line.  $T_0$  is found to be  $\sim 18,000$ K.

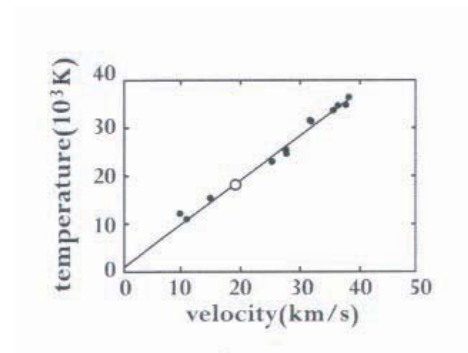


Fig.9. Velocity vs temperature,  $\tau(T) / \tau(T_0) = \alpha(v) / \alpha(v_0)$ . The standard point by the u-photomultiplier is shown by (o). The solid line is a guide for the eye.

Therefore, the amplitude  $\alpha(v) / \alpha(v_0)$  should be measured using only samples of category I. By extrapolating these points to zero amplitude using the u-photomultiplier, the threshold velocity  $v_0$  was estimated to be  $\sim 19$  km/s as shown in Fig.8. This value corresponds to  $T_0$  of  $\sim 18,000$ K.

By applying the same procedure to the signal forms from the b-photomultiplier, these quantities are found to be  $\sim 11,000$  K and  $\sim 11$  km/s. By using the relation  $\tau(T) / \tau(T_0) = \alpha(v) / \alpha(v_0)$ , they are found to be  $\sim 12,000$  K and  $\sim 10$  km/s, respectively, for the  $v_1$ -photomultiplier.

The relationship  $\tau(T) / \tau(T_0) = \alpha(v) / \alpha(v_0)$  is two-dimensionally plotted in Fig.9 The temperature-velocity relationship appears slightly concave-up in shape. Here the relationship may be approximated to be linear in the velocity range from 10 to 40 km/s. Thus, the conversion rate was estimated to be  $\sim 900$  K/km/s. This conversion rate was much higher than that reported earlier [4,5]. This conversion rate is to be reevaluated by considering the influence of secondary particles generated during collision.

In summary, the proposed method is useful for measuring the temperature immediately after collision of hypervelocity microparticles with solid materials. The conversion rate  $\sim 900$  K/km/s was obtained with an error of 30% in the range of 10 – 40 km/s. This value was found to be much higher than that reported earlier. This was considered as the screening effect due to secondary particles.

#### References

- [1] T.Miyachi et al, Appl. Phys. Lett. **93**, 174107 (2008).
- [2] T.Miyachi et al., J. Appl. Phys. **98**, 014110, 2005.
- [3] T.Miyachi et al., Jpn J. Appl. Phys. **47**, 3772, 2008.
- [4] G.Eichhorn, Planet Space Sci. **23**, 1519, 1975.
- [5] G.Eichhorn, Planet Space Sci. **26**, 463, 1978.